

Article

# Numerical Analysis of Blood Clot Mechanical Behavior in Relation to Blood Flow Inside the Popliteal Vein

Mantas Brusokas <sup>1</sup> and Raimondas Jasevičius <sup>1,2,3,\*</sup>

<sup>1</sup> Department of Mechanics and Materials Engineering, Vilnius Gediminas Technical University, Plytinės Str. 25, 10105 Vilnius, Lithuania; mantas.brusokas@vilniustech.lt

<sup>2</sup> Institute of Mechanical Science, Vilnius Gediminas Technical University, Plytinės Str. 25, 10105 Vilnius, Lithuania

<sup>3</sup> Department of Biomechanical Engineering, Faculty of Mechanics, Vilnius Gediminas Technical University, Plytinės Str. 25, 10105 Vilnius, Lithuania

\* Correspondence: raimondas.jasevicius@vilniustech.lt

**Abstract:** In this work, blood clot behavior under the influence of the mechanical effect of blood flow was analyzed. Attention is mainly paid to the deformation of the thrombus in the event of an alternating effect of blood flow in the blood vessel of the human leg. It is assumed that the higher stress accumulation is associated with a decrease in the width of the lumen of the blood vessel. The idea is to represent a critical case when embolus can form. The geometry of the thrombus is selected on the basis of existing blood patterns. Modeling is performed using COMSOL Multiphysics software. The results reflect the distribution of stress and blood velocity over time. The work selected a critical case, when the formation of an embolus is possible due to the deformation of the thrombus by the blood flow. Research is important for studying the behavior of thrombus formation at different periods of time, and also taking into account the specific geometry of thrombus deformation for the purpose of predicting embolisms. The results are observed due to increased deformations in the appropriate areas of the clot, whose tests show specific blood deformation from the alternating effects of blood on different sections of the vessels.

**Keywords:** blood clot; vessel; mechanics; stress strain; COMSOL Multiphysics

**MSC:** 37M05; 37M10; 37N15; 70K40; 74H15; 92B05; 92C05; 92C10



**Citation:** Brusokas, M.; Jasevičius, R. Numerical Analysis of Blood Clot Mechanical Behavior in Relation to Blood Flow Inside the Popliteal Vein. *Mathematics* **2024**, *12*, 267. <https://doi.org/10.3390/math12020267>

Academic Editors: Ionuț Gabriel Ghionea, Cristian Ioan Tarbă and Saša Čuković

Received: 14 December 2023

Revised: 9 January 2024

Accepted: 12 January 2024

Published: 14 January 2024



**Copyright:** © 2024 by the authors. Licensee MDPI, Basel, Switzerland. This article is an open access article distributed under the terms and conditions of the Creative Commons Attribution (CC BY) license (<https://creativecommons.org/licenses/by/4.0/>).

## 1. Introduction

Blood clot analysis, since it is itself composed of and influenced by many factors, can be observed from different perspectives. The literature in this field can be divided into seven main areas: blood clots; veins; mechanics, stress strain; modelling; methodologies and methods; and poro-viscoelastic behavior. First, we would like to discuss the first of these areas of research, blood clots. The fluid mechanics of blood clot formation were analyzed by Fogelson and Neeves [1]. They found that intravascular blood clots form in an environment in which hydrodynamic forces dominate. The engineering design of optimal strategies for blood clot dissolution was analyzed by Diamond [2]. He established that blood clots form under hemodynamic conditions. The treatment of blood clots was analyzed by Goldhaber and Grasso-Correnti [3]. They found that blood clots in the veins or venous system can cause deep venous thrombosis. The basic principles and clinical practice for the treatment of hemostasis and thrombosis were provided by Colman et al. [4]. Practical hemostasis and thrombosis treatment methods were presented by Key et al. [5].

In addition, it is also important to mention studies related to atrial fibrillation in the left atrium, which show that stagnant blood flow can cause the formation of blood clots (Corti et al. [6]). As the blood clot ages, the density and size of the fibrin threads change

on the surface and in the core of the blood clot, the distribution of RBCs becomes more uniform, and their concentration increases (Zhou et al. [7]).

Next, we would like to discuss works related to veins. Deep venous thrombosis was analyzed by Olaf and Cooney [8]. They argued that the treatment depends on individual conditions, but usually consists of anticoagulation for a finite or infinite period of time, depending on the suspected etiology of the thrombosis. Also, deep vein thrombosis was analyzed by Thachil [9]. He argued that slow movement of the blood in the circulation is commonly caused by immobility.

Continuing our review of blood clot studies, it is worth mentioning the blood clot analysis from the point of view of mechanics, as well as stress strain. Nonlinear, dissipative phenomena in the mechanics of whole blood clots were analyzed by Sugerman et al. [10]. They demonstrated that thrombus resistance to embolization is driven by its intrinsic fracture toughness as well as other non-surface-creating dissipative mechanisms. To establish the mechanical properties of blood clots, a test method was presented by Krasokha et al. [11]. They performed compressive strength experiments on aged human blood clots. A new compressible hyperelastic model for the multi-axial deformation of blood clot occlusions in vessels was presented by Fereidoonzhad et al. [12]. They noted that mechanical thrombectomy can be significantly affected by the mechanical properties of the occluding thrombus. The tensile and compressive mechanical behavior of human blood clot analogues was examined by Cahalane et al. [13]. They argued that endovascular thrombectomy procedures are significantly influenced by the mechanical response of thrombi to the multi-axial loading imposed during retrieval. The nanomechanics of blood clot and thrombus formation were presented by Domingues et al. [14]. They produced a review providing an outline of the building mechanisms for blood clots' mechanical properties and how they relate to clot function. The rupturing of blood clots, including its mechanics and pathophysiology, was studied by Tutwiler et al. [15]. In order to obtain the critical behavior of the clot, they added an edge crack to the blood clot under consideration. In vivo measurement of blood clot mechanics from computational fluid dynamics based on intravital microscopy images was undertaken by Kadri et al. [16]. They performed a mechanical analysis of a clot, which had a smooth, peak-free geometry. They argued that at the same time, the viscoplastic behavior exhibited by thrombi resembles that of a Bingham plastic—a material similar to toothpaste that behaves as a rigid body at low stresses but flows as a viscous fluid when its critical yield stress is exceeded.

We would next like to pay attention to studies concerning blood clot-related modeling/simulation. Spatial stabilization strategies applied to the Multiphysics modeling of blood clotting using a modified Phan–Thien–Tanner (PTT) model were presented by Egger et al. [17]. Their work focused on a stabilization strategy to circumvent the numerical difficulties experienced when applying the PTT model to a more complex aneurysm geometry. Simulation studies for the non-invasive classification of ischemic and hemorrhagic stroke using near-infrared spectroscopy were performed by Ahirwar et al. [18]. Their simulation studies showed the pressure on the blood vessel walls under ischemic and hemorrhagic stroke conditions and also that under a nominal blood flow velocity, hemorrhaging does not occur, but when the velocity is sufficient enough to increase the pressure on the wall, the rupturing of the mid-cerebral artery takes place. Recent advances in computational modeling of thrombosis are given by Yesudasan and Averett [19]. They reviewed the recent developments in the area of computational modeling of blood clot formation using various methods at different length and time scales. Model predictions of deformation, embolization and permeability of partially obstructive blood clots under variable shear flow were presented by Xu et al. [20]. Their simulations provide new insights into the mechanisms underlying clot stability and embolization that cannot be studied experimentally at this time. A blood clot simulation model using the bond-graph technique was presented by Romero et al. [21]. They found that the shorter the length, the lower the time needed to extract the clot, because it has less adherence force and less inertia due to the mass. The matrix orientation model was presented by Dallon et al. [22].

Next, we would like to discuss studies covering methodologies and methods. Numerical methods for simulating blood flow at the macro, micro, and multi scales were given by Imai et al. [23]. They mentioned that numerical methods in the computational biomechanics of blood flow may be classified by the type of computational mesh used for the fluid domain into fixed mesh methods, moving mesh (boundary-fitted mesh) methods, and mesh-free methods. Systems analysis of thrombus formation was performed by Diamond [24]. He mentioned that common numerical tools include the finite element method, immersed boundary elements, lattice Boltzmann, Monte Carlo, and dissipative particle dynamics. Multiscale modeling of blood flow-mediated platelet thrombosis was performed by Yazdani et al. [25]. They described multiscale numerical methodologies that integrate four key components of blood clotting, namely coagulation kinetics and the transport of species, blood rheology, cell mechanics, and platelet adhesive dynamics, across a wide range of spatiotemporal scales. Analysis of blood flow in compliant vessels was carried out by Čanić et al. [26]. They used ultrasound measurements and Doppler methods to detect the wall behavior and fluid velocity. A whole blood thrombus mimic was presented by Sugerman et al. [27]. They mentioned that thrombi are not regularly shaped and make testing via standard methods difficult.

Finally, we would like to discuss studies examining poro-viscoelastic behavior. The viscoporoelasticity of coagulated blood clots was investigated by He et al. [28]. They argued that the particular viscoporoelastic properties of a coagulated blood clot can be related to many factors, such as the volume fraction of platelets, the fibrin concentration, the erythrocyte count, the thrombin concentration, and so on. A blood clot behaves as a poro-visco-elastic material, as shown by Ghezlbash et al. [29]. They argued that neither the poroelastic nor viscoelastic theories alone could explain the full spectrum of relaxation behavior of blood clots. The viscoelasticity of blood in the non-clotting and clotting states and its clinical significance were investigated by Ikemoto and Isogai [30]. They mentioned that the changes in viscoelasticity during the coagulation process have been observed in various diseases. Finite element analysis of blood clots based on the nonlinear visco-hyperelastic model was performed by Tashiro et al. [31]. They found that by incorporating viscoelastic theory into the FEM, typical characteristics of clots such as stress relaxation and the strain rate and hysteresis characteristics could be computationally reproduced. Phase transitions during the compression and decompression of clots from platelet-poor plasma, platelet-rich plasma and whole blood were investigated by Liang et al. [32]. They found that the viscoelastic response and hysteresis behavior of compressed and uncompressed clots suggest that there are changes in clot structure, depending on the degree and rate of compression.

In the present introduction, the importance of studying thrombi/blood clots is evident, and thus the relevance of this study is high. In general, in the theoretical model presented in the current work, we do not add cracks in the structure of the blood clot, but we choose the structure/geometry of the blood clot with certain peaks, where the probability of embolism formation is high. To provide more detail about this study, its foundations are presented in the next section, entitled 'Problem Formulation'.

## 2. Problem Formulation

In general, our scientific research is divided into two main directions. The first is associated with the mechanical processes that occur inside the cell (e.g., DNA mechanics). The second relates to the mechanics of cells/viruses (e.g., RBCs, platelets, bacteria, coronaviruses) and structures (e.g., blood clots) consisting of cells. In this work, we followed the second direction, examining the mechanical behavior of the blood clot.

Understanding the mechanical processes in the blood vessel itself, which affect the thrombus, can be beneficial to public health. Diseases that are related to the heart and the circulatory system are one of the main causes of death, responsible for more than 3.9 million deaths a year in Europe (Wilkins et al. [33]). In the known literature, there is not much knowledge of how the physical thrombus formation process takes place over

time. As a result, numerical studies remain important. According to the results of physical experiments in the known literature, this work aims to learn more about the mechanical effects of force and stress, as well as providing an analysis of stress values that occur on the surface of blood clots using input parameters. This work applied the computational fluid dynamics (CFD) method to describe the mechanical forces and stresses that affect blood clots in blood vessels during blood flow. Also, the mechanical processes inside blood vessels that affect the possible rupture of the thrombus are analyzed. In further experiments, it would be useful to analyze the mechanical processes that take place inside a blood vessel when it is blocked an embolus.

In this work, a blood clot is considered as a linear elastic solid, although the introduction presents well-known works showing that a blood clot can also be considered as a poroviscoelastic material. A blood clot, like most biological tissues, has both viscoelasticity and poroelasticity, and Ghezelbash et al. [29] proved that blood clots are poroviscoelastic. According to He et al. [28], the poroelastic and viscoelastic processes of a blood clot allow it to dissipate energy, which contributes to delaying the fracturing of the blood clot. In our proposed model, we analyze blood clots as a linear elastic solid using corresponding parameters of the clot, which allows us to calculate stresses influenced by the blood flow. Naturally, the poroviscoelasticity would reduce the energy received, which would consequently delay the fracturing, yet the aim of the work was to increase our understanding of how the blood flow influences blood clots.

At this stage of the problem, the provided model is sufficient, as we are replicating the geometry established in the literature. Moreover, *in vivo*, it is difficult to extract the exact geometry of the thrombus in a safe way, because the ultrasound imaging method does not provide an accurate enough result and intravital microscopy is not practiced on human blood clots yet. It is important to note that according to Kadri et al. [16], there are some discrepancies between *ex vivo* and *in vivo* measurements. The aim of our work is to examine blood clots with the geometry observed in the known literature, which is continuously changing. The assumed geometry has probes that allow not only the separation of the whole thrombus from the wall of the vessel, but also venous thromboembolism (VTE) when the thrombus is partially split.

It should also be mentioned that various blood clot processes are known, and each of them requires a separate analysis—such a study would cover more than one publication/investigation. In order to realize this difficult task, it is necessary to take the first step, namely analyzing the deformation of blood clots. Without this step, further research would be difficult/inappropriate, as the entire task is too complex to be solved (considering the nanonewton or even piconewton scale, Jasevičius [34–36]) by today's computers. As an example, modeling the interactions between single cells forming a blood clot requires an infinitesimally small time step (0.3 picosecond time step, Jasevičius [34–36]). It is known that a blood clot consists of not only red blood cells (Jasevičius [34,35]), but also platelets (Jasevičius [36]), white cells, as well as the fibrin meshwork. It is known that the red blood cell (RBC) count is 4 to 6 million cells per cubic millimeter, and if we estimate the time it takes for a blood clot to form and the motion of millions of composing parts (the different geometries of the pseudopodia containing activated platelets, fibrinogen and erythrocytes, and the movement of the composing parts during blood flow) that could make up the clot, as well as the different forms of blood clots, we can establish that modeling the formation of a blood clot using today's computer resources would be a very difficult or even unsolvable task currently. Therefore, inevitably, this task is idealized, with the purpose of taking the first step in this effort. The purpose of this study conditionally covers all of the above cases, given that the corresponding part of the blood clot has already been formed over the same period of time as the corresponding structure for modeling (needed for possible embolus identification), when modeling includes the proper level of idealization. Additional sticking/involvement of blood cells is not considered. As mentioned earlier, the formation of a blood clot requires a time that can last from 4 to 10 min, and if it concerns the formation of a thrombus, this can last for weeks or even years (Czaplicki et al. [37]). As already mentioned,

the first step is to examine the deformation of blood clots, which is an important point of analysis in this stage of this study. Without understanding the mechanics of blood clots, it would be difficult to determine/understand the mechanics of the possible phenomena related to the formation of embolisms.

As mentioned earlier, this article presents a critical case in which embolus formation can be expected. We would like to point out that the detachment of the embolus from the blood vessel is still unclear from a mechanical point of view, and initial studies are needed to elucidate this complex process. The numerical implementation itself requires additional analysis. In the next section, we to introduce the simulation tool that we used in our calculations.

### 3. Methodology

A single formed blood clot located inside a vessel, which was based on in vivo and ex vivo blood clot geometry experiments [1,38], was modeled and drawn using COMSOL Multiphysics (software version 5.5; developer location: 100 District Avenue, Burlington, MA 01803, USA). Even though a blood clot consists of various different particles, in this article, it was considered as a solid isotropic body.

For this experiment, the clot was drawn with a length of around 12 mm and a height of around 6.5 mm. Its uneven shape was designed to match a possible real-life scenario.

As seen in Figure 1, the clot was placed inside a  $\text{Ø}12$  mm vein with a length of 30 mm. This research work focused solely on the mechanical processes of the clot, so the pulsations and deformations of the vein were not considered. Therefore, all of the outside walls inside the software (inlet, top/bottom and outlet) were considered as a fixed geometry. The mesh was generated by the software using a sequence type of Fluid-Structure Physics-controlled mesh.

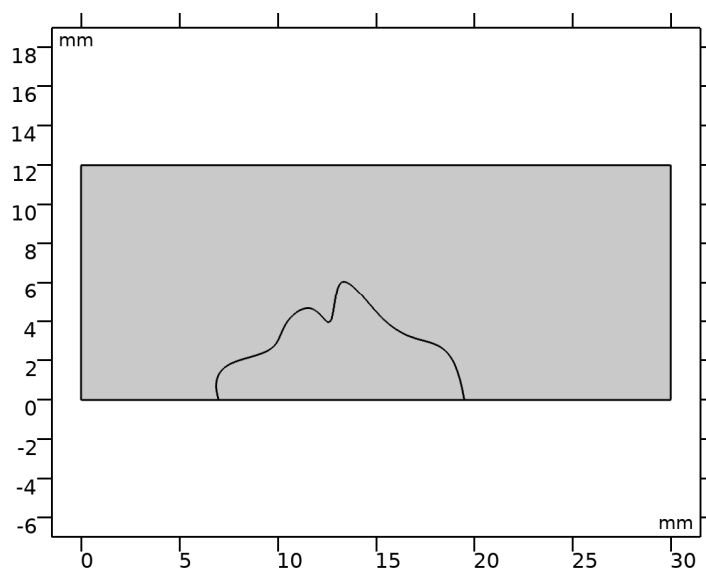


**Figure 1.** Clot in vessel. Full simulation model (created using COMSOL Multiphysics software).

The element size was fine, and the mesh consisted of 7199 elements, mostly triangles, but quads and edge elements can also be seen in Figure 2. The exact location of the thrombus was taken to be set in the human popliteal vein, and the clot had the corresponding parameters. The initial parameters are given in Table 1.

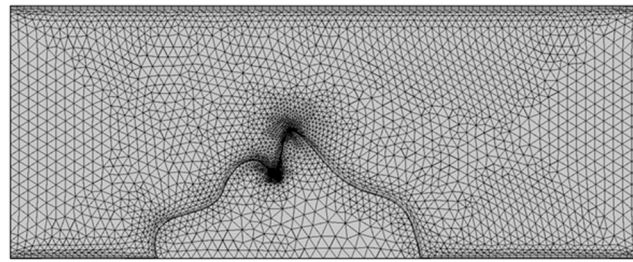


Figure 2. Meshed simulation model (created using COMSOL Multiphysics software).

Table 1. Initial parameters for simulation [39–42].

	Density	Dynamic Viscosity	Young’s Modulus	Poisson’s Ratio
Blood	1060 kg/m <sup>3</sup>	4 cP (mPa·s)	-	-
Blood Clot	1100 kg/m <sup>3</sup>	-	1.5 kPa	0.48

It is important to note that venous blood flow is not constant, i.e., venous blood flow varies from person to person [43,44], and it also varies over time within the same individual due to natural fluctuations in limb flow [43–45]. The pattern of blood flow varies depending on the specific physiology and position of the body at a given time, as respiration and the cardiac cycle modulate blood flow to varying degrees [43,44]. In addition, the blood pressure in the veins is constantly changing; therefore, the reproducibility of blood flow velocity in a particular vein of an individual over time is not possible [43]. In this case, a graph of potential pulsatile blood flow velocity with a peak velocity greater than 20 cm/s was plotted [43,46]. Gravity and negative flows were not evaluated due to the valves inside the vein.

For all simulations, the input velocity was used as shown in Figure 3, imitating P75 heartbeats per minute. Also, the following boundary conditions were set: the inflow boundary condition was fully developed flow; outflow boundary condition—0 pressure and suppressed backflow; wall and blood clot boundary condition—no slip; fluid–structure interaction: the fixed geometry coupling type was fully coupled.

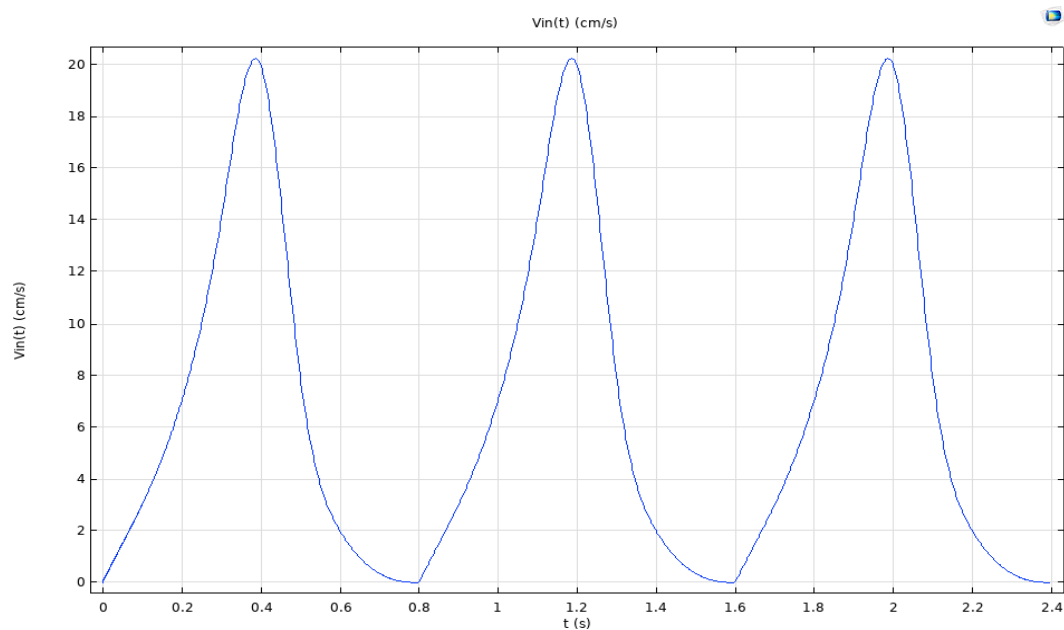


Figure 3. Change in the blood flow velocity over a certain period of time (created using COMSOL Multiphysics software).

Numerical simulation was based on the Navier–Stokes equation [47]:

$$\rho_b \left( \frac{\delta \mathbf{v}}{\delta t} + \mathbf{v} \cdot \nabla \mathbf{v} \right) = -\nabla p + \nabla \cdot \left( \mu \left( \nabla \mathbf{v} + (\nabla \mathbf{v})^T \right) - \frac{2}{3} \mu (\nabla \cdot \mathbf{v}) \mathbf{I} \right) + \mathbf{F} \quad (1)$$

where  $\mathbf{v}$  is the velocity of the fluid (blood),  $p$  is the pressure of the fluid (blood),  $\rho_b$  is the density of the fluid (blood), and  $\mu$  is the dynamic viscosity of the fluid (blood). These equations are always solved together with the continuity equation:

$$\frac{\delta \rho_b}{\delta t} + \nabla \cdot (\rho_b \mathbf{v}) = 0 \quad (2)$$

Depending on the flow regime of interest, these equations can often be simplified. For incompressible flows, the continuity equation gives:

$$\nabla \cdot \mathbf{v} = 0 \quad (3)$$

Since the velocity divergence is zero, the following term is also zero:

$$-\frac{2}{3} \mu (\nabla \cdot \mathbf{v}) \quad (4)$$

It can therefore be removed from the viscous force term in the N–S Equation (1) in the case of an incompressible flow.

The stresses were calculated using the momentum balance equation, which in terms of the Cauchy stress tensor can be written as [47]:

$$\rho_{bc} \frac{\partial^2 \mathbf{u}}{\partial t^2} = \mathbf{f}_v + \nabla_x \cdot \boldsymbol{\sigma} \quad (5)$$

where  $\rho_{bc}$  is the density of the blood cloth,  $\mathbf{u}$  is displacement field,  $\boldsymbol{\sigma}$  is the Cauchy stress tensor, and  $\mathbf{f}_v$  is volumetric force (force per deformed volume). It is important to note here that density in this equation characterizes the true density of the deformed material.

The density partly appertains on the deformation due to the mass conservation as:

$$\rho_{bc} = J^{-1} \rho_{bc0} \quad (6)$$

where  $J$  is volume factor, which provides the volume change caused by the deformation.

By using the velocity and modifying the independent variables into spatial coordinates via  $x = x(X, t)$ :

$$\rho_{bc} \left[ \frac{\partial \mathbf{v}}{\partial t} + (\mathbf{v} \cdot \nabla_x) \mathbf{v} \right] = \mathbf{f}_v + \nabla_x \cdot \boldsymbol{\sigma} \quad (7)$$

This is the momentum balance in the Eulerian formulation. This formulation is used in fluid dynamics, where the velocity is assessed as a dependent variable.

The stress power is the rate of change in the strain energy density, and the stress power for an elastic material can be represented as:

$$\int_V \boldsymbol{\sigma} : \mathbf{L} dV = \int_{V_0} \mathbf{P} : \dot{\mathbf{F}} dV_0 \quad (8)$$

where tensor  $\mathbf{P}$  is the first Piola–Kirchhoff stress tensor,  $\mathbf{F}$  is the deformation gradient tensor, and  $V_0$  is undeformed material volume.

Velocity gradient can be disintegrated into symmetric and antisymmetric parts, which are called the strain rate tensor ( $\mathbf{L}_d$ ) and spin tensor ( $\mathbf{L}_w$ ). Considering that the Cauchy stress tensor is symmetric:

$$\boldsymbol{\sigma} : \mathbf{L} = \boldsymbol{\sigma} : \mathbf{L}_d \quad (9)$$

Therefore, the strain measure that is the power conjugated to the Cauchy stress is the strain rate tensor. It can also be written as:

$$L_d = F^{-T} \dot{E} F^{-1} \tag{10}$$

where

$$E = \frac{1}{2} (F^T F - I) \tag{11}$$

where  $E$  is the Green–Lagrange strain tensor, while  $I$  is the identity tensor. Then, the stress power integral could be reworked as:

$$\int_V \sigma : L_d dV = \int_{V_0} S : \dot{E} dV_0 \tag{12}$$

Here

$$S = J F^{-1} \sigma F^{-T} \tag{13}$$

This is called the second Piola–Kirchhoff stress tensor. It is a symmetric tensor that is the energy conjugated to the Green–Lagrange strain. The first and second Piola–Kirchhoff stress tensors are connected via:

$$P = F S = (I + \nabla \mathbf{u}) S \tag{14}$$

This equation allows us to rewrite the momentum balance equation as:

$$\rho_{bc0} \frac{\partial^2 \mathbf{u}}{\partial t^2} = F_v + \nabla_x \cdot [(I + \nabla \mathbf{u}) S] \tag{15}$$

which, conjointly with a constitutive relation of the form

$$S = S(E), \tag{16}$$

will provide an enclosed system of equations for the displacement vector.

In this paper, we analyzed blood clots as linear elastic solid materials, while the viscoelastic rheology equations are also provided [47]. For a linear elastic material, Hooke’s law relates the stress tensor to the elastic strain tensor:

$$\sigma = \sigma_{ex} + C : \varepsilon_{el} = \sigma_{ex} + C : (\varepsilon - \varepsilon_{inel}) \tag{17}$$

where  $C$  is the 4th-order elasticity tensor, and ‘:’ stands for the double-dot tensor product (or double contraction). The elastic strain  $\varepsilon_{el}$  is the difference between the total strain  $\varepsilon$  and all inelastic strains  $\varepsilon_{inel}$ . There may also be an extra stress contribution  $\sigma_{ex}$  with contributions from initial stresses and viscoelastic stresses. However, for isotropic linear elastic materials in the absence of inelastic stresses, Hooke’s law in Equation (17) reduces to:

$$\sigma = \sigma_{ex} + C : \varepsilon_{el} \tag{18}$$

Using the generalized Maxwell model, the total stress in Hooke’s law (18) is modified and then augmented by the viscoelastic stress  $\sigma_q$ :

$$\sigma = \sigma_0 + C : \varepsilon_{el} + \sigma_q \tag{19}$$

In this case, viscoelastic stress  $\sigma_q$  is the sum of the stresses in the viscoelastic branches and is computed from:

$$\sigma_q = \sum_{m=1}^N \sigma_m = \sum_{m=1}^N 2G_m (\varepsilon - \gamma_m) \tag{20}$$

where  $G_m$  represents the stiffness in the branch and the auxiliary variable  $\gamma_m$  represents extensions in the dashpots.

#### 4. Results

Analysis of the mechanical deformations of the thrombus was performed using numerical simulation performed using the COMSOL Multiphysics software. Mechanical changes in the blood clot are predicted by varying fluid inlet velocities. The whole domain is shown in the following figures, representing the cross section of a  $\varnothing 12$  mm popliteal vein with a length of 30 mm. The simulation results are presented in five time steps, 1.02 s, 1.10 s, 1.18 s, 1.26 s and 1.34 s, respectively.

First, we would like to address the first timestamp at 1.02 s, which is 0.22 s after the start of the period. For this and the following figures, the white-teal-blue coloring indicates the blood velocity in cm/s, the green-red coloring indicates the amount of displacement of the blood clot in mm, black streamlines (arrow lines) with triangles denote the velocity field, and three white dots indicate the local maxima: (a) blood clot stress according to von Mises in  $\text{N/m}^2$ ; (b) the value of the speed of blood movement in cm/s; and (c) the magnitude of the displacement of the blood clot in mm.

According to Figure 4, at the 1.02 s instance, the blood flow reaches and begins to pass the position of the clot. The initial blood flow velocity is slightly increasing, but, because of the narrowing of the vessel, the blood flow velocity at the thrombus section is already quite high (maximum local value  $v_1 = 21.63$  cm/s). This velocity is already enough to start deforming the protruding thrombus parts (maximum local value  $u_1 = 0.3005$  mm). Insignificant stresses at the bottom of the protruding part can be noticed (maximum local value  $\sigma_1 = 205.55$   $\text{N/m}^2$ ). Most of the blood is exiting the 30 mm cross section of the vein, but some signals of flow anomalies are forming.

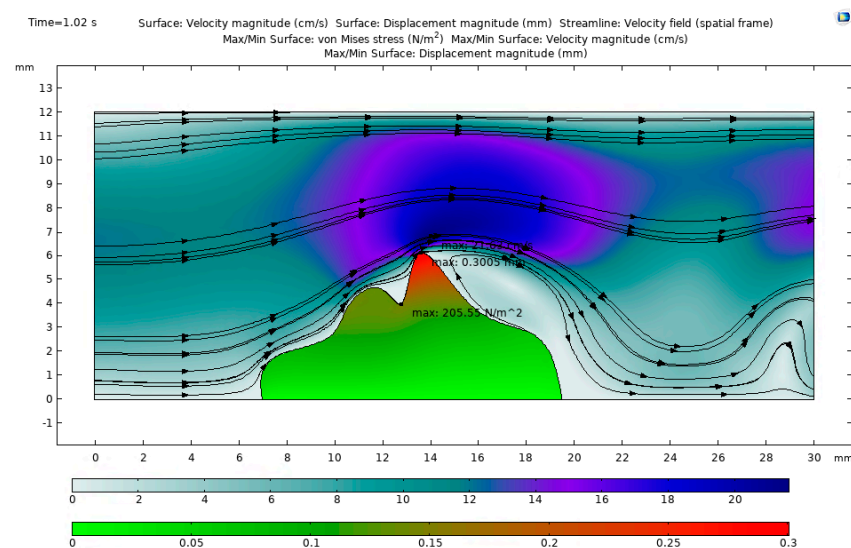


**Figure 4.** Blood flow and blood clot interaction at the 1.02 s time step (created using COMSOL Multiphysics software, considering Equations (1)–(20)).

In Figure 5 (at time instance 1.10 s), the clot continues to act as an obstacle and reduces the internal area of the vessel, and hence the velocity increases even more (maximum local value  $v_2 = 36.17$  cm/s). The clot deforms even more (maximum local value  $u_2 = 0.7119$  mm), which leads to an increase in stress at the bottom of the deformable part of the thrombus (maximum local value  $\sigma_2 = 808.86$   $\text{N/m}^2$ ). Signs of blood flow vortex formation can be seen just behind the clot.

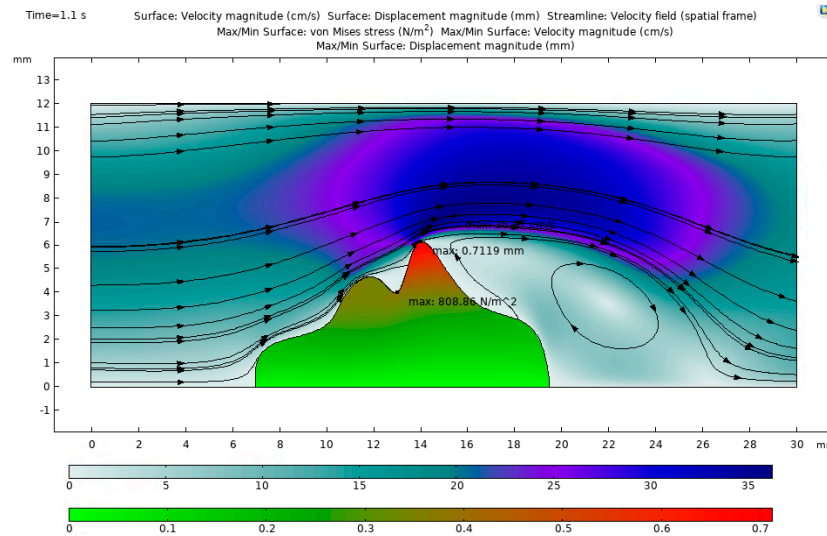


**Figure 5.** Blood flow and blood clot interaction at the 1.10 s time step (created using COMSOL Multiphysics software, considering Equations (1)–(20)).

In Figure 6 (at time instance 1.18 s), the main blood flow is passing or has already passed the position of the clot. The blood flow velocity has reached its maximum values and with further movement through the vein begins to decrease somewhat due to the restoration of the normal cross-sectional area (maximum local value  $v_3 = 53.33$  cm/s). At this moment, maximum deformation of the upper part of the thrombus occurs (maximum local value  $u_3 = 1.238$  mm), causing maximum stress in the lower part of the deformable section of the thrombus (maximum local value  $\sigma_3 = 11960$  N/m<sup>2</sup>). Due to this spike, depending on the composition of the clot, clot rupture and the detachment of part of it (embolus formation) may occur. Some of the outgoing blood begins to create a noticeable vortex.

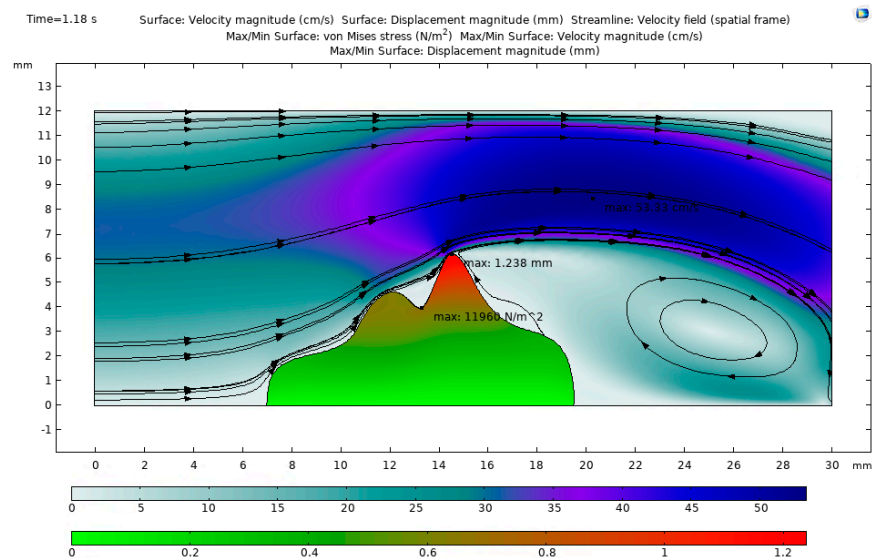


**Figure 6.** Blood flow and blood clot interaction at the 1.18 s time step (created using COMSOL Multiphysics software, considering Equations (1)–(20)).

After only 0.08 s of the previous time stamp (Figure 7, at time instance 1.26 s), the prime blood flow passes the clot and the velocity decreases in the narrow cross-sectional area of the thrombus, yet the maximum local value ( $v_4 = 47.51$  cm/s) is still high as the flow is leaving the vessel. The most deformed place of the clot returns to its original

position (maximum local value  $u_4 = 0.3927$  mm). The stress drops drastically (maximum local value  $\sigma_4 = 370.17$  N/m<sup>2</sup>). Significant blood flow vortexes are obtained.

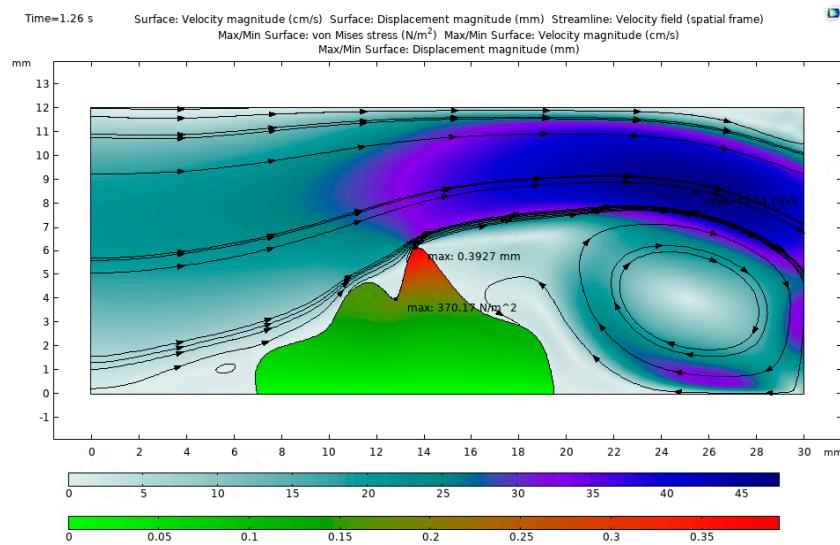


**Figure 7.** Blood flow and blood clot interaction at the 1.26 s time step (created using COMSOL Multiphysics software, considering Equations (1)–(20)).

In Figure 8, the last time stamp of 1.34 s, which is 0.54 s after the start of the period, is examined. The main blood flow has completely passed the site of the clot at this point. The blood flow velocity decreases (maximum local value  $v_5 = 27.45$  cm/s). The Whole clot returns to its initial position and is almost totally non-deformed (maximum local value  $u_5 = 0.01273$  mm). The stress has also almost fully been relieved (maximum local value  $\sigma_5 = 12.623$  N/m<sup>2</sup>). The exiting blood turns in a vortex shape before moving further through the circulatory system.

Also, according to well-known experiments performed by Fereidoonzhad et al. [12,48] and Cahalane et al. [13], our results show that the distribution of stress is likely in the range of 0–60 kN/m<sup>2</sup>, depending on % RBC value, for the thrombus, while in our experiment, it was found to be 0–12 kN/m<sup>2</sup>. Additional further studies are needed when it comes to the numerical implementation of embolism process.

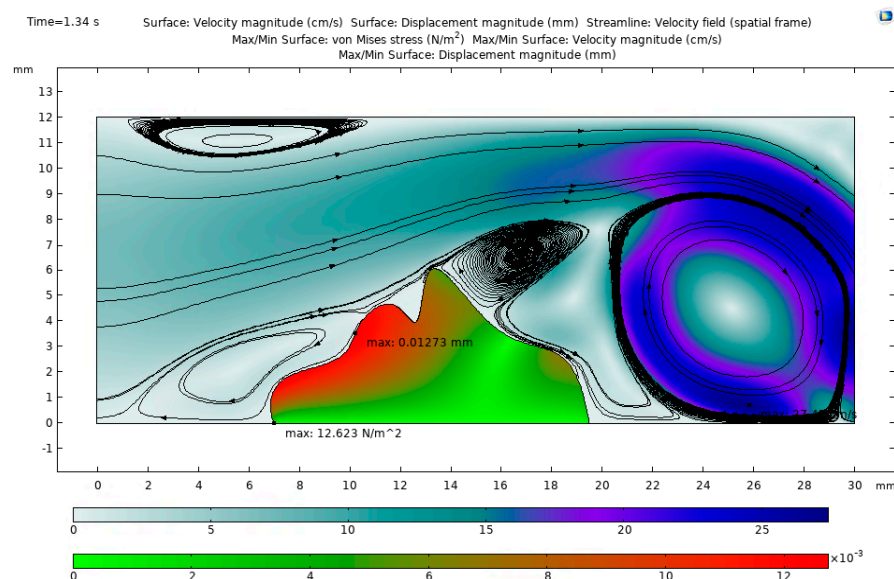


**Figure 8.** Blood flow and blood clot interaction at the 1.34 s time step (created using COMSOL Multiphysics software, considering Equations (1)–(20)).

## 5. Discussion

We followed a different path, because during coagulation, the clot increases in size and at each moment of time it has a different shape and size. We took a relevant time period (throughout its life span) and examined its biomechanical properties over this period. Moreover, we chose the exact time interval after which the clot would likely detach from the vessel surface or embolize (we chose a critical case that would be relevant for physicians, since it is the most difficult for them to determine when surgical intervention is necessary). The shape of the embolus and the mechanical properties affecting it, after evaluating the diameter of the blood vessel accordingly, are important factors determining the possibility of thrombus detachment.

The deformations are observed throughout the blood flow due to the properties of the soft material, which allows the blood clot to deform as the blood flows. However, as the results show, the greatest stresses are observed only in the upper part of the thrombus. The stresses varied widely (0–12 kN/m<sup>2</sup>), but this study, as a first step, aimed to find out what theoretically possible stresses occur in a thrombus with a corresponding shape. During this study, the form of the thrombus was selected for which the formation of an embolus is likely.

When analyzing the displacement values of the deformable body of the thrombus from the initial moment of time, a push of the apex of the thrombus up to 1.3 mm is observed. Therefore, it is believed that this size will influence the formation of the curvature of the thrombus apex. Both displacement and peak stresses could have a decisive influence on the separation of the clot apex from the thrombus.

It should be noted that the results also show the formation of vortices behind the thrombus. Compared to the maximum observed blood velocity, the blood flow velocity in the area behind the clot is approximately 10 times slower. For example, from the known physical experiments performed by Gonzalo et al. [49], Aguado et al. [50], and Pasta et al. [51], it is known that the cause of the formation of a blood clot is a slowdown in blood flow in the left atrium of the heart (appendicitis). Therefore, we hypothesize that in our study, this phenomenon of slower blood flow could conceivably contribute to faster thrombus formation (additional formation of a larger thrombus was not examined in this work).

Figures 4–8 show the different distribution of blood flow behind the clot. We would like to mention that this can depend on many factors, for example stenosis, the geometry of the blood clot, etc. These mentioned factors can affect changes in blood flow. Due to this, we would now like to discuss additional works in which this phenomenon is presented. Flow effects on coagulation and thrombosis were analyzed by Hathcock [52]. He argued that after the stenosis, fluid layers may separate from one another as it decelerates, forming stagnation zones and areas of recirculation. The structure of a shear-induced platelet aggregated clot formed in an *in vitro* arterial thrombosis model was investigated by Kim and Ku [53]. After a physical experiment (*in vitro*), they found that the growing thrombus at the apex alters the flow environment and creates a larger recirculation region downstream. Endothelial shear stress in the evolution of coronary atherosclerotic plaque and vascular remodeling was studied by Wentzel et al. [54]. They found that blood flow may resemble a disturbed laminar flow, characterized by areas of flow reversal (i.e., flow separation, recirculation, and reattachment to the forward flow).

Although there are many publications in the literature that examine blood clots using a porous viscoelastic model, the question remains as to whether this is the only suitable model to describe the behavior of blood clot material. If we look at a blood clot not as a single body, but as an object consisting of individual components (red blood cells [34,35], platelets [36], and fibrin), it becomes important to examine the forces that act on each individual component of a blood clot [34–36]. According to previous studies [34–36,55], for the cell, the influence of adhesion force becomes important, as well as energy dissipation associated with a change in the influence of adhesion during interaction with the surface. Meanwhile, the viscous damping model is more suitable for describing the sticking process

of the cell to the surface [35,55]. In addition, this model of viscous damping is used to describe internal friction and dissipation of energy, when the energy is dissipated into heat due to internal friction. As was mentioned previously, the energy dissipation can also occur due to changes in the effect of adhesion [34–36,55]. The adhesive forces for the attached cell play an important role, since the cell should remain stuck to the surface of the blood clot or remain stuck inside the blood clot, forming the internal structure of the blood clot. It is important to note that the blood clot in the process of its formation changes its shape, reacts to blood flow, and also has residual deformations as a heterogeneous material (also nonhomogeneous or inhomogeneous material); therefore, elastic–plastic deformation, as well as the associated mechanism of energy dissipation, should be taken into account [55].

After evaluating previously expressed remarks and based on previous single-cell studies, the model of elastic deformation was chosen as the first step in this work, and subsequently, more complex models will be considered in the future as further steps in studying blood clot mechanics. Also, in further studies, we hope to evaluate the possible formation of an embolus when the material (blood clot) fails to withstand the stress in the corresponding part of the clot and a part of the clot detaches. An additional study of the recirculation and stagnation of blood flow is also necessary in the future. Additionally, the key findings are presented below:

#### *Key Findings*

- The geometry of the blood clot has a direct effect on the formation of an embolism. It was noted that the highest stresses are concentrated around the formed peaks of a blood clot. Due to high stress, the separation of part of the blood clot/peak (embolus) can be expected.
- Due to the thrombus, at different time intervals, the different recirculation process and the recirculation “center” location can be expected. The stagnation of blood flow near the blood clot surface was also observed. It is known that the stagnation of blood flow in the left atrial appendage can lead to the formation of a blood clot. In our case, we assume that the stagnation of blood flow in the blood vessel leads to acceleration of the thrombus formation process.
- Due to changes in the lumen of the blood vessel (stenosis), a higher concentration of stress and blood flow velocity can be expected; these criteria can lead to damage to the blood vessel (popliteal vein aneurysm) and the surrounding tissue.

## 6. Conclusions

This work investigated the mechanical behavior of a thrombus in the presence of blood flow and heart rate in the corresponding time interval. During the numerical experiment, various phenomena are observed: clot deformation, uneven stress distribution, changes in blood flow, and the formation of vortices. After analyzing the clot with the considered shape, we can say that the geometry of the thrombus plays a significant role in embolization, especially when the thrombus has a corresponding protrusion. As a thrombus forms and the lumen of the blood vessel decreases, the thrombus protrudes due to increased blood flow velocity and is subject to the highest mechanical stresses. Increased deformation and the resulting stress create a favorable environment for embolization. In future research, we will consider embolism itself. This may occur when parts of a blood clot separates from the rest of the blood clot or when the entire blood clot separates from the surface of the blood vessel.

**Author Contributions:** Conceptualization, methodology, investigation, writing—original draft preparation M.B. and R.J. All authors have read and agreed to the published version of the manuscript.

**Funding:** This research received no external funding.

**Data Availability Statement:** Data are contained within this article.

**Conflicts of Interest:** The authors declare no conflicts of interest.

## Nomenclature

CFD	computational fluid dynamics;
DVT	deep venous thrombosis;
RBC	red blood cell;
VTE	venous thromboembolism;
<i>Roman</i>	
$v$	blood velocity (cm/s);
$u$	deformation of the clot (mm);
$p$	pressure of the fluid (Pa);
$f_v$	volumetric force (N);
$J$	volume factor;
$P$	first Piola–Kirchhoff stress tensor;
$F$	deformation gradient;
$V_0$	undeformed material volume (m <sup>3</sup> );
$E$	Young’s modulus (Pa);
<i>Greek</i>	
$\sigma$	blood clot stresses (N/m <sup>2</sup> );
$\rho_b$	density of the fluid (blood) (kg/m <sup>3</sup> );
$\rho_{bc}$	density of the blood clot (kg/m <sup>3</sup> );
$\mu$	dynamic viscosity of the fluid (cP);
$\varepsilon$	total strain;
$\nu$	Poisson’s ratio.

## References

1. Fogelson, A.L.; Neeves, K.B. Fluid Mechanics of Blood Clot Formation. *Annu. Rev. Fluid Mech.* **2015**, *47*, 377–403. [[CrossRef](#)] [[PubMed](#)]
2. Diamond, S.L. Engineering Design of Optimal Strategies for Blood Clot Dissolution. *Annu. Rev. Biomed. Eng.* **1999**, *1*, 427–461. [[CrossRef](#)] [[PubMed](#)]
3. Goldhaber, S.Z.; Grasso-Correnti, N. Treatment of blood clots. *Circulation* **2002**, *106*, 138–140. [[CrossRef](#)] [[PubMed](#)]
4. Marder, V.J.; Aird, W.C.; Bennett, J.S.; Schulman, S.; White, G.C., II; Colman, R.W.; Hirsh, J.; Marder, V.J.; Clowes, M.D.; Alexander, W.; et al. (Eds.) *Hemostasis and Thrombosis: Basic Principles and Clinical Practice*, 5th ed; Lippincott Williams & Wilkins: Philadelphia, PA, USA, 2006; 1827p.
5. Key, N.; Makris, M.; O’Shaughnessy, D.; Lillicrap, D. *Practical Hemostasis and Thrombosis*, 2nd ed.; Wiley-Blackwell: Oxford, UK, 2009.
6. Corti, M.; Zingaro, A.; Dede, L.; Quarteroni, A.M. Impact of Atrial Fibrillation on Left Atrium Haemodynamics: A Computational Fluid Dynamics Study. *Comput. Biol. Med.* **2022**, *150*, 106143. [[CrossRef](#)] [[PubMed](#)]
7. Zhou, Y.; Murugappan, S.K.; Sharma, V.K. Effect of clot aging and cholesterol content on ultrasound-assisted thrombolysis. *Transl. Stroke Res.* **2014**, *5*, 627–634. [[CrossRef](#)]
8. Olaf, M.; Cooney, R. Deep Venous Thrombosis. *Emerg. Med. Clin. N. Am.* **2017**, *35*, 743–770. [[CrossRef](#)]
9. Thachil, J. Deep vein thrombosis. *Hematology* **2014**, *19*, 309–310. [[CrossRef](#)]
10. Sugerman, G.P.; Parekh, S.H.; Rausch, M.K. Nonlinear, dissipative phenomena in whole blood clot mechanics. *Soft Matter* **2020**, *16*, 9908–9916. [[CrossRef](#)]
11. Krasokha, N.; Theisen, W.; Reese, S.; Mordasini, P.; Brekenfeld, C.; Gralla, J.; Slotboom, J.; Schrott, G.; Monstadt, H. Mechanical properties of blood clots—A new test method. *Mater. Werkst.* **2010**, *41*, 1019–1024. [[CrossRef](#)]
12. Fereidoonnehad, B.; Moerman, K.M.; Johnson, S.; McCarthy, R.; McGarry, P.J. A new compressible hyperelastic model for the multi-axial deformation of blood clot occlusions in vessels. *Biomech. Model Mechanobiol.* **2021**, *20*, 1317–1335. [[CrossRef](#)]
13. Cahalane, R.M.E.; de Vries, J.J.; de Maat, M.P.M.; van Gaalen, K.; van Beusekom, H.M.; van der Lugt, A.; Fereidoonnehad, B.; Akyildiz, A.C.; Gijzen, F.J.H. Tensile and compressive mechanical behaviour of human blood clot analogues. *Ann. Biomed. Eng.* **2023**, *51*, 1759–1768. [[CrossRef](#)] [[PubMed](#)]
14. Domingues, M.M.; Carvalho, F.A.; Santos, N.C. Nanomechanics of blood clot and thrombus formation. *Annu. Rev. Biophys.* **2022**, *51*, 201–221. [[CrossRef](#)] [[PubMed](#)]
15. Tutwiler, V.; Singh, J.; Litvinov, R.I.; Bassani, J.L.; Purohit, P.K.; Weisel, J.W. Rupture of blood clots: Mechanics and pathophysiology. *Sci. Adv.* **2020**, *6*, eabc0496. [[CrossRef](#)] [[PubMed](#)]
16. Kadri, O.E.; Chandran, V.D.; Surblyte, M.; Voronov, R.S. In vivo measurement of blood clot mechanics from computational fluid dynamics based on intravital microscopy images. *Comput. Biol. Med.* **2019**, *106*, 1–11. [[CrossRef](#)] [[PubMed](#)]
17. Egger, J.; Mallik, A.S.; Szczerba, D.; Ruefenacht, D.A.; Szekely, G.; Hirsch, S. Spatial stabilization strategies applied to Multiphysics modeling of blood clotting using a modified PTT model. *Procedia Comput. Sci.* **2013**, *18*, 996–1005. [[CrossRef](#)]

18. Ahirwar, D.; Shakya, K.; Banerjee, A.; Khurana, D.; Chowdhury, S. Simulation studies for non invasive classification of ischemic and hemorrhagic stroke using near infrared spectroscopy. *Biodevices* **2019**, *1*, 192–198. [CrossRef]
19. Yesudasan, S.; Averett, R.D. Recent advances in computational modeling of fibrin clot formation: A review. *Comput. Biol. Chem.* **2019**, *83*, 107148. Available online: <https://www.researchgate.net/publication/322328874> (accessed on 28 September 2023). [CrossRef]
20. Xu, S.; Xu, Z.; Kim, O.V.; Litvinov, R.I.; Weisel, J.W.; Alber, M. Model predictions of deformation, embolization and permeability of partially obstructive blood clots under variable shear flow. *J. R. Soc. Interface* **2017**, *14*, 20170441. [CrossRef]
21. Romero, G.; Martinez, M.L.; Maroto, J.; Felez, J. Blood clot simulation model by using the Bond-Graph technique. *Sci. World J.* **2013**, *2013*, 519047. [CrossRef]
22. Dallon, J.C.; Sherratt, J.A.; Maini, P.K. Mathematical modelling of extracellular matrix dynamics using discrete cells: Fiber orientation and tissue regeneration. *J. Theor. Biol.* **1999**, *199*, 449–471. [CrossRef]
23. Imai, Y.; Omori, T.; Shimogonya, Y.; Yamaguchi, T.; Ishikawa, T. Numerical methods for simulating blood flow at macro, micro, and multi scales. *J. Biomech.* **2016**, *49*, 2221–2228. [CrossRef] [PubMed]
24. Diamond, S.L. Systems Analysis of Thrombus Formation. *Circ. Res.* **2016**, *118*, 1348–1362. [CrossRef] [PubMed]
25. Yazdani, A.; Zhang, P.; Sheriff, J.; Slepian, M.J.; Deng, Y.; Bluestein, D. Multiscale modeling of blood flow-mediated platelet thrombosis. In *Handbook of Materials Modeling: Applications: Current and Emerging Materials*; Andreoni, W., Yip, S., Eds.; Springer: Cham, Germany, 2018; pp. 1–32. [CrossRef]
26. Čanić, S.; Hartley, C.J.; Rosenstrauch, D.; Tambača, J.; Guidoboni, G.; Mikelić, A. Blood flow in compliant arteries: An effective viscoelastic reduced model, numerics, and experimental validation. *Ann. Biomed. Eng.* **2006**, *34*, 575–592. [CrossRef] [PubMed]
27. Sugeran, G.P.; Kakaletsis, S.; Thakkar, P.; Chokshi, A.; Parekh, S.H.; Rausch, M.K. A whole blood thrombus mimic: Constitutive behavior under simple shear. *J. Mech. Behav. Biomed.* **2021**, *115*, 104216. [CrossRef] [PubMed]
28. He, D.; Kim, D.A.; Ku, D.N.; Hu, Y. Viscoporoelasticity of coagulation blood clots. *Extreme Mech. Lett.* **2022**, *56*, 101859. [CrossRef]
29. Ghezlbash, F.; Liu, S.; Shirazi-Adl, A.; Li, J. Blood clot behaves as a poro-visco-elastic material. *J. Mech. Behav. Biomed. Mater.* **2022**, *128*, 105101. [CrossRef]
30. Ikemoto, S.; Isogai, Y. S20.6. Viscoelasticity of blood in the non-clotting and clotting states, and its clinical significance. *Biorheology* **1995**, *32*, 181. [CrossRef]
31. Tashiro, K.; Shobayashi, Y.; Ota, I.; Hotta, A. Finite element analysis of blood clots based on the nonlinear visco-hyperelastic model. *Biophys. J.* **2021**, *120*, 4547–4556. [CrossRef]
32. Liang, X.; Chernysh, I.; Purohit, P.K.; Weisel, J.W. Phase transitions during compression and decompression of clots from platelet-poor plasma, platelet-rich plasma and whole blood. *Acta Biomater.* **2017**, *60*, 275–290. [CrossRef]
33. Wilkins, E.; Wilson, L.; Wickramasinghe, K.; Bhatnagar, P.; Leal, J.; Luengo-Fernandez, R.; Burns, R.; Rayner, M.; Townsend, N. European cardiovascular disease statistics. In *European Cardiovascular Disease Statistics*; European Heart Network: Brussels, Belgium, 2017. Available online: <https://www.bhf.org.uk/informationsupport/publications/statistics/european-cardiovascular-disease-statistics-2017> (accessed on 28 September 2023).
34. Jasevičius, R. Numerical modeling of red blood cell interaction mechanics. *Mech. Adv. Mater. Struct.* **2023**, *30*, 2524–2531. [CrossRef]
35. Jasevičius, R. Numerical modelling of erythrocyte sticking mechanics. *Appl. Sci.* **2022**, *12*, 12576. [CrossRef]
36. Jasevičius, R. Numerical modeling of thrombocyte interaction mechanics with a blood vessel wall. *Mathematics* **2023**, *11*, 4814. [CrossRef]
37. Czaplicki, C.; Albadawi, H.; Partovi, S.; Gandhi, R.T.; Quencer, K.; Deipolyi, A.R.; Oklu, R. Can thrombus age guide thrombolytic therapy? *Cardiovasc. Diagn. Ther.* **2017**, *7*, S186–S196. [CrossRef] [PubMed]
38. Hwang, J.Q.; Kimberly, H.H.; Liteplo, A.S.; Sajed, D. An evidence-based approach to emergency ultrasound. *Emerg. Med. Pract.* **2011**, *13*, 1–27. [PubMed]
39. Sadowska, A.; Spodnik, J.H.; Wojcik, S. Variations in popliteal fossa venous anatomy: Implications for diagnosis of deep-vein thrombosis. *Folia Morphol.* **2013**, *72*, 51–56. [CrossRef] [PubMed]
40. Mfoumou, E.; Tripette, J.; Blostein, M.; Cloutier, G. Time-dependent hardening of blood clots quantitatively measured in vivo with shear-wave ultrasound imaging in a rabbit model of venous thrombosis. *Thromb. Res.* **2013**, *133*, 265–271. [CrossRef] [PubMed]
41. Wang, S.H.; Lee, L.P.; Lee, J.S. A linear relation between the compressibility and density of blood. *Acoust. Soc. Am.* **2011**, *109*, 390–396. [CrossRef]
42. Kenner, T. The measurement of blood density and its meaning. *Basic Res. Cardiol.* **1989**, *84*, 111–124. [CrossRef]
43. Morris, R.J.; Woodcock, J.P. Evidence-based compression. *Ann. Surg.* **2004**, *239*, 162–171. [CrossRef]
44. Fronek, A.; Criqui, M.H.; Denenberg, J.; Langer, R.D. Common femoral vein dimensions and hemodynamics including Valsalva response as a function of sex, age, and ethnicity in a population study. *J. Vasc. Surg.* **2001**, *33*, 1050–1056. [CrossRef]
45. Lewis, P.; Psaila, J.V.; Davies, W.T.; McCarty, K.; Woodcock, J.P. Measurement of volume flow in the human common femoral artery using a duplex ultrasound system. *Ultrasound Med. Biol.* **1986**, *12*, 777–784. [CrossRef] [PubMed]
46. Hitos, K.; Cannon, M.; Cannon, S.; Garth, S.; Fletcher, J.P. Effect of leg exercises on popliteal venous blood flow during prolonged immobility of seated subjects: Implications for prevention of travel—Related deep vein thrombosis. *J. Thromb. Haemost.* **2007**, *5*, 1890–1895. [CrossRef] [PubMed]

47. *CFD Module User's Guide*; COMSOL: Burlington, MA, USA, 2018. Available online: <https://doc.comsol.com/5.4/doc/com.comsol.help.cfd/CFDModuleUsersGuide.pdf> (accessed on 28 September 2023).
48. Fereidoonzehad, B.; Dwivedi, A.; Johnson, S.; McCarthy, R.; McGarry, P. Blood clot fracture properties are dependent on red blood cell and fibrin content. *Acta Biomater.* **2021**, *127*, 213–228. [[CrossRef](#)] [[PubMed](#)]
49. Gonzalo, A.; García-Villalba, M.; Rossini, L.; Durán, E.; Vigneault, D.; Martínez-Legazpi, P.; Flores, O.; Bermejo, J.; McVeigh, E.; Kahn, A.M.; et al. Non-Newtonian blood rheology impacts left atrial stasis in patient-specific simulations. *Int. J. Numer. Method Biomed. Eng.* **2022**, *38*, e3597. [[CrossRef](#)] [[PubMed](#)]
50. Aguado, A.M.; Olivares, A.L.; Yagüe, C.; Silva, E.; Nuñez-García, M.; Fernandez-Quilez, A.; Mill, J.; Genua, I.; Arzamendi, D.; De Potter, T.; et al. In silico optimization of left atrial appendage occluder implantation using interactive and modeling tools. *Front. Physiol.* **2019**, *10*, 237. [[CrossRef](#)] [[PubMed](#)]
51. Pasta, S.; Guccione, J.M.; Kassab, G.S. Inversion of left atrial appendage will cause compressive stresses in the tissue: Simulation study of potential therapy. *J. Pers. Med.* **2022**, *12*, 883. [[CrossRef](#)] [[PubMed](#)]
52. Hathcock, J.J. Flow effects on coagulation and thrombosis. *Arterioscler. Thromb. Vasc. Biol.* **2006**, *26*, 1729–1737. [[CrossRef](#)]
53. Kim, D.A.; Ku, D.N. Structure of shear-induced platelet aggregated clot formed in an in vitro arterial thrombosis model. *Blood Adv.* **2022**, *6*, 2872–2883. [[CrossRef](#)]
54. Wentzel, J.J.; Chatzizisis, Y.S.; Gijssen, F.J.; Giannoglou, G.D.; Feldman, C.L.; Stone, P.H. Endothelial shear stress in the evolution of coronary atherosclerotic plaque and vascular remodelling: Current understanding and remaining questions. *Cardiovasc. Res.* **2012**, *96*, 234–243. [[CrossRef](#)]
55. Jasevičius, R.; Kruggel-Emden, H. Numerical modelling of the sticking process of a *S. aureus* bacterium. *Int. J. Adhes. Adhes.* **2017**, *77*, 15–28. [[CrossRef](#)]

**Disclaimer/Publisher's Note:** The statements, opinions and data contained in all publications are solely those of the individual author(s) and contributor(s) and not of MDPI and/or the editor(s). MDPI and/or the editor(s) disclaim responsibility for any injury to people or property resulting from any ideas, methods, instructions or products referred to in the content.